13 (2026) 17–24

Contents lists available at ScienceDirect

Deep Brain Stimulation

journal homepage: www.journals.elsevier.com/deep-brain-stimulation

Paradoxical targeting: Overlap between optimal and gait-impairment stimulation sites in essential tremor

Anouk A. Boogaard [a], Maarten Bot [b], Yarit Wiggerts [b], Martijn Beudel [a], Rick Schuurman [b], Rob M.A. de Bie [a], Arthur W.G. Buijink [a,*]

[a] Department of Neurology, Amsterdam University Medical Center, Amsterdam Neuroscience, University of Amsterdam, Amsterdam, the Netherlands
[b] Department of Neurosurgery, Amsterdam University Medical Center, Amsterdam Neuroscience, University of Amsterdam, Amsterdam, the Netherlands

ARTICLE INFO

Keywords:
Essential Tremor
Deep brain stimulation – gait
Dentato-rubro-thalamic tract

ABSTRACT

Background: Deep brain stimulation (DBS) is an effective treatment for medication-refractory essential tremor (ET), typically targeting the ventral intermediate nucleus (VIM), posterior subthalamic area (PSA), or dentato-rubro-thalamic tract (DRTT). However, up to one-third of patients develop gait impairment, possibly due to stimulation of unintended or overlapping pathways. This study investigated stimulation areas specifically linked to tremor improvement and gait impairment.

Methods: We retrospectively analyzed clinical data from 40 ET patients (80 hemispheres) treated with DBS. Tremor improvement was assessed with the Fahn-Tolosa-Marin (FTM) tremor rating scale and gait impairment was assessed with the first item of the Scale for Assessment and Rating of Ataxia (SARA). Volume of tissue activated (VTA) were modeled using Lead-DBS and voxel-wise associations were examined with Spearman-rank correlations. Mixed effects regression was used to evaluate clinical and stimulation-related covariates.

Results: Regions linked to both tremor reduction and gait impairment overlapped with the VIM, PSA, and DRTT ($p < 0.05$, FDR corrected). No distinct region was exclusively associated with gait impairment. Stimulation location was not statistically significant related to postoperative gait outcome. Patients with more severe baseline gait ataxia were more likely to deteriorate, although this association was not statistically significant after bootstrapping.

Conclusion: Our findings suggest that DBS may simultaneously engage therapeutic and adverse pathways within the DRTT. A potential somatotopic organization of the cortico-thalamo-cerebellar (CTC) network may underlie this overlap, though it could not be disentangled in this study. Future work integrating individual functional connectivity and tractography may help delineate specific pathways, enabling more precise targeting and improved outcomes for ET patients.

1. Introduction

Essential Tremor (ET) is one of the most prevalent movement disorders [1]. In medication-refractory ET, deep brain stimulation (DBS) can reduce tremor by up to 90% [2]. The effect of DBS in ET is thought to result from modulation of the cerebello-thalamo-cortical (CTC) network [3,4]. The optimal stimulation target, however, remains controversial. Some studies suggest that the ventral intermediate nucleus (VIM) of the thalamus is most effective, whereas others propose the posterior subthalamic area (PSA), consisting of the caudal zona incerta and prelemniscal radiation [5,6]. Both areas are connected to the dentato-rubro-thalamic tract (DRTT), a major pathway within the CTC network [4]. Proximity of electrode contact points to this tract have been significantly associated with improved tremor suppression [7,8].

Although DBS can be highly effective in reducing tremor, its benefits may be offset by DBS-induced ataxia. In a large retrospective cohort study one third of ET patients experienced DBS-induced ataxia, including dysarthria and gait impairment [9]. Post-operative gait impairment has been linked to stimulation of the VIM, PSA and DRTT [10,11]. Furthermore, DBS-induced gait impairment may be related to specific stimulation parameters or unintended overlap of the stimulation field with nearby structures. For instance, gait ataxia has been

* Correspondence to: Department of Neurology, Amsterdam University Medical Centers, Amsterdam Neuroscience, University of Amsterdam, PO-Box 22660, Amsterdam 1100DD, the Netherlands.
E-mail address: a.w.buijink@amsterdamumc.nl (A.W.G. Buijink).

https://doi.org/10.1016/j.jdbs.2026.05.001
Received 22 January 2026; Accepted 3 May 2026
Available online 5 May 2026

associated with stimulation closer to the posteromedial border of the subthalamic nucleus (STN) [10]. Moreover, higher stimulation amplitudes may activate adjacent white matter tracts, potentially leading to ataxia [12,13]. Antidromic overactivation of the cerebellum and stimulation of non-crossing DRTT fibers have also been proposed as potential mechanisms [14]. These findings suggest that while effective tremor suppression relies on optimal stimulation within the CTC network, DBS-induced ataxia may reflect suboptimal targeting within this network or stimulation settings that inadvertently engage adjacent structures.

Previous studies have extensively investigated the optimal regions for tremor suppression; however, the stimulation sites underlying side effects, particularly gait impairment, remain less well understood [7,15]. Furthermore, gait disturbances are often considered a subset of ataxia, but emerging evidence suggests that distinct stimulation regions – potentially overlapping with the PSA – may specifically contribute to gait dysfunction [11]. Notably, prior investigations have not directly associated the volume of tissue activated (VTA) with gait impairment. While some studies have compared mean VTA locations between ET patients with and without ataxia, none have conducted voxel-wise analyses correlating individual normalized VTA regions with quantitative measures of gait dysfunction in order to localize stimulation areas linked to adverse effects [10,15]. The objective of this study is to delineate specific stimulation areas associated with gait impairment on group level. We hypothesize that gait impairment and tremor improvement are mediated by distinct stimulation sites in the (sub)thalamic area.

2. Methods

2.1. Patients

In this retrospective study data was collected and analyzed from a cohort comprising 54 ET patients who have undergone DBS-surgery at Amsterdam University Medical Center between Januari 2010 and April 2020. An opt-out procedure was applied in accordance with institutional and national guidelines. Implanted DBS systems are Boston Vercise Cartesia™ (directional lead, Boston Scientific, Marlborough, MA, USA) and Medtronic Activa™ (electrode lead model 3389, Medtronic, Minneapolis, MN). Inclusion criteria were implantation of bilateral electrodes, availability of complete preoperative and postoperative MR- and CT-imaging for studying anatomical relations and precise electrode position after implantation, availability of tremor scores and video recordings of a gait assessment at the pre-operative assessment and post-operative follow-up (after 6–12 months).

2.1.1. Clinical outcomes

Tremor severity was evaluated using the Fahn-Tolosa-Marin Tremor Rating Scale (FTM-TRS) at screening prior to DBS-surgery and during follow-up 6–12 months after DBS surgery [16]. Percentage improvement scores are calculated for each hemisphere with items from the FTM part A and B assessing upper and lower extremity tremor. Additionally, gait impairment was scored retrospectively from video recordings at intake and follow-up sessions with the Scale for Assessment and Rating of Ataxia (SARA) item 1, score range 0–8 [17]. For this item subjects were asked to walk 10 m including a half turn and perform a tandem walk (heels to toes) without support. Gait assessment was scored blinded for stimulation condition by an experienced neurologist (A.B.). A worsening of ≥ 1 was labeled as DBS-induced gait impairment to capture clinically relevant deterioration. Furthermore, data pertaining to any additional comorbidities, disease duration, (tremor) medication usage and stimulation parameters at follow-up were collected. Total electrical energy delivered (TEED) was calculated as a general measure for stimulation as some patients had current-controlled DBS systems and others voltage-controlled DBS systems. To calculate TEED, first current was converted to voltage with Ohm's law, and subsequently the formula $TEED = (V^2 \bullet f \bullet pw)/R$ was used [18,19]. Since there were no impedance values available a typical impedance of 1000 Ω was used [18].

2.2. Imaging

Preoperative 3D T1-weighted magnetic resonance imaging (MRI) scans were acquired using a 3 T Elition Ingenia scanner (Philips, Best, The Netherlands) with 32-channel receive coil (repetition time (TR)= 8.81 ms, echo time (TE)= 4.03 ms, echo train length (ETL)= 242, field of view (FOV)= 256x256x170 mm, voxel size = 0.25 × 0.25 × 1 mm, scan time = 8 min. After electrode implantation, an intraoperative stereotactic O-arm cone-beam computed tomography scan (Medtronic, Inc.) was acquired with a slice thickness of 0.83 mm, and an in-plane resolution of 0.41 × 0.41 mm (FOV= 20 cm, 192 slices, 120 kV, 150 mAs, scan time 30 s) [20].

2.3. DBS electrode localization

DBS electrodes are localized employing the processing pipeline in Lead-DBS version 3.0 (leaddbs.org; RRID:SCR_002915) [21,22]. Preoperative T1-weighted 3 T MRI scans were linearly co-registered to post-operative CT scans using Advanced Normalization Tools (ANTs [23]). In cases where ANTs failed due to enlarged ventricles, FMRIB's Linear Image Registrations Tool (FLIRT) was employed as an alternative registration method [24]. Pre- (and post-) operative acquisitions were spatially normalized into MNI152NLin2009bAsym space based on pre-operative T1-weighted MRI using the SyN registration approach as implemented in ANTs [23]. DBS electrodes were automatically pre-localized in native and template space using the PaCER algorithm and manually adjusted if necessary [25]. DBS electrodes were localized in MNI space and transformed to anterior commissure-posterior commissure (ACPC) coordinates with the ACPC/MNI conversion tool of Lead-DBS with origin the mid commissural point (MCP) or PC of the AC-PC line [26].

For each electrode E-field distribution and volume of tissue activated (VTA) were calculated using the OSS-DBS algorithm as implemented in Lead-DBS with a threshold of 0.2 V/mm. This algorithm takes tissue heterogeneity, anisotropy and different axonal morphologies into account, and uses adaptive mesh refinement, parallel processing, and frequency-based computational methods. The areas that have a field strength above the threshold of 0.2 V/mm are part of the VTA. VTAs in the left hemisphere were flipped to the right hemisphere using non-linear mirroring. The *Sweetspot explorer* in Lead DBS was used to calculate an N-image by summing the number of times each voxel was covered by a VTA. Only voxels that were covered by at least 4 VTAs were included in the analyses. Mean images were then generated for both tremor improvement and gait impairment by summing the clinical outcomes for each voxel and dividing it by the number of VTAs covering that voxel.

2.4. Stimulation location

Stimulation locations were identified by an experienced neurosurgeon (M.B.) through detailed evaluation of FGATIR, T1-weighted structural MRI scans and electrode reconstructions within the Brainlab Elements software (Brainlab AG, Munich, Germany), to determine whether the active contact resided within the VIM or the PSA [27]. These stimulation locations were compared to the location of active contact points in FGATIR MNI space in Lead DBS. The distance to the DRTT was calculated as described in Dembek et al. [7]. The DRTT was taken from the probabilistic atlas of Dembek et al. (thresholded at $p \geq 0.5$) in MNI152NLin2009bAsym space. Active contact coordinates were localized in MNI space and compared to the DRTT in each hemisphere. For each contact, we computed a local, probability-weighted center of gravity (COG) of the DRTT within a ± 1 mm slab around the

contact's z-coordinate. To calculate the distance between the active contact points and closest center of gravity Euclidean distances were calculated.

2.5. Statistical analysis

Descriptive statistics for baseline characteristics and tremor scores were computed using MATLAB (version R2020b, The MathWorks, Inc., Natick, MA, USA). Normality was assessed using Shapiro-Wilk tests and visual inspection of distributions. Mean and standard deviation are reported for normally distributed outcomes, median and interquartile range from the first quartile (25th percentile) to the third quartile (75th percentile) for non-normally distributed outcomes.

2.5.1. Stimulation maps

Two stimulation maps were calculated and visualized, displaying voxels significantly associated with more tremor improvement or greater gait disturbance. Spearman's rank correlation is used to assess the relationship between stimulation at each voxel and the outcome of interest (tremor improvement or gait impairment). The resulting correlation coefficients are transformed into t-statistics and tested voxel-wise using a Wilcoxon signed-rank test to generate a statistical log10 (p)-map. This p-map represents the confidence level of the association between voxel stimulation and tremor improvement or gait impairment.

The Wilcoxon test was performed under two null hypotheses. First, a null hypothesis of zero was used to identify significant voxel clusters associated with tremor improvement or gait disturbance. Second, a null hypothesis of the mean clinical outcome was applied to determine an area, where stimulation leads to greater improvement or greater impairment compared to other voxels. To correct for multiple testing, a false discovery rate (FDR) correction was applied, and p-values below 0.05 were considered significant. The Essential Tremor Probabilistic Mapping atlas and the average DRTT from Dembek et al. were used to visualize electrode positions, N-maps, and significance maps in relation to anatomical structures involved in ET [7,15].

2.5.2. Stimulation parameters and clinical outcomes

The relation between stimulation location and gait impairment and tremor improvement was further explored with mixed effect models. To account for the non-independence of observations arising from bilateral electrode placements within individuals, mixed effects models with a random intercept for each participant were employed using RStudio (RStudio Team, 2023), with a significance level of $p < .05$ [28]. The first model examined a binary outcome reflecting gait impairment (categorized as "no gait deterioration" vs. "gait deterioration") using a logistic mixed-effects regression. Fixed effects included age (log-transformed and standardized), baseline gait scores (square-root transformed and standardized), stimulation location (PSA vs. VIM) and distance to DRTT (in mm).

The second model addressed the continuous outcome of tremor improvement, modeled using a linear mixed effects regression with log-transformed tremor improvement scores as the dependent variable. The same set of predictors and random effect structure were included. To ensure robust estimation of confidence intervals for the fixed effects in the gait impairment model, parametric bootstrapping with 1000 resamples was performed. This was chosen to provide more accurate confidence intervals given the low variance and hierarchical structure of the data. Given the exploratory nature of this study, no corrections for multiple comparisons were applied for the regression analyses.

To avoid overfitting, TEED was excluded from these main models. Instead we evaluated its relation with gait and tremor improvement in separate models, including age, baseline gait scores, and tremor improvement or gait impairment as covariates.

3. Results

3.1. Clinical characteristics

Forty patients were included from our cohort of 54 patients. Four patients were excluded due to unilateral DBS, two due to missing follow-up data and eight due to poor data quality of pre- or postoperative imaging. In four included patients follow-up videos were missing and therefore gait assessment was possible in 36 patients Table 1 shows clinical characteristics of the included patients. Eighty VTAs (2 hemispheres per patient) were analyzed. Tremor improvement varied between participants from −20–100% per hemisphere, data was slightly skewed to the left (skewness= −0.40) indicating a tendency toward higher tremor reduction values and followed a non-normal distribution ($W=0.96$, $p = 0.005$). Gait impairment scores range from 0 to 3, are slightly skewed to the right (skewness= 0.72) and not normally distributed ($W=0.83$, $p < 0.001$), which shows a tendency toward lower gait impairment values (see Fig. 1 and Supplementary material).

Values are presented as mean + /- SD or median (IQR) or n (%). Tremor improvement is expressed as percentage change from baseline. Active contact coordinates are shown in mm in the right-anterior-superior (RAS) convention. Coordinates from the left hemisphere were flipped to the right hemisphere. FTM-TRS = Fahn-Tolosa-Marin Tremor Rating Scale, Hz = Herz, mA = milliampere, MCP = mid-commissural point, μs = microseconds, PC = posterior commissure, SARA = Scale for the Assessment and Rating of Ataxia, TEED = Total Electrical Energy Delivered (microjoules/s).

3.2. Stimulation maps

The N-map, representing the combined stimulation volumes (VTAs) across patients is depicted in Fig. 2A/B. This aggregate volume covers part of the VIM and extends into the PSA, including structures such as the caudal zona incerta and the prelemniscal radiation. Notably, the N-map also overlaps with the posterior portion of the stimulation "sweet spot" (shown in yellow) previously published by Nowacki et al. [15].

Fig. 3 shows the results of a voxel-wise analysis performed under the null hypothesis of zero, which revealed significant stimulation maps associated with tremor improvement and DBS-induced gait impairment ($p < 0.05$, FDR-corrected). The resulting stimulation maps encompass overlapping regions, primarily localized on the ventral aspect of the VIM, medial-posterior region of the STN, and are located more lateral, not overlapping with the RN. Regions significantly associated with tremor improvement (2A-C) and gait impairment (2D-F) overlap with the VIM and PSA and DRTT. Voxels with the strongest statistical

Table 1
Clinical and stimulation characteristics of the study cohort (N = 40).

Age (years) (n = 40)	75 (68.75 – 77)
Sex (female) (n = 40)	18 (45%)
Pre-FTM TRS (80 hemispheres)	54 (46.25 – 63)
Post-FTM TRS (80 hemispheres)	19.5 (14 – 29.25)
Tremor improvement % (80 hemispheres)	53.39% (31.05– 75)
Right (40 hemispheres)	50% (24.81 – 62.38)
Left (40 hemispheres)	69.78% (36.67 – 83.67)
Gait score pre-DBS (SARA item 1, n = 36)	1 (0 – 1)
Gait-score post-DBS (SARA item 1, n = 36)	1.50 (1 – 2)
Gait-score difference (post – pre, n = 36)	1 (0 – 1)
DBS-induced gait impairment (worsening ≥ 1, n = 36)	N = 19 (54%)
Stimulation amplitude (mA, 72 hemispheres)	1.8 (1.5 – 2.55)
Stimulation frequency (Hz, 80 hemispheres)	130 (130 – 154)
Stimulation pulse width (μs, 80 hemispheres)	60 (60 – 60)
TEED (microjoules/s, 72 hemispheres)	31.12 (19.36 – 49.56)
Mean active contact (in mm, 80 hemispheres)	
X coordinate, mm lateral from mid-AC-PC	12.96 (SD 2.05)
Y coordinate, mm anterior to PC	6.44 (SD 1.94)
Z coordinate, relative to AC-PC line	-0.85 (SD 2.72)
Stimulation location PSA/VIM (72 hemispheres)	13 / 59

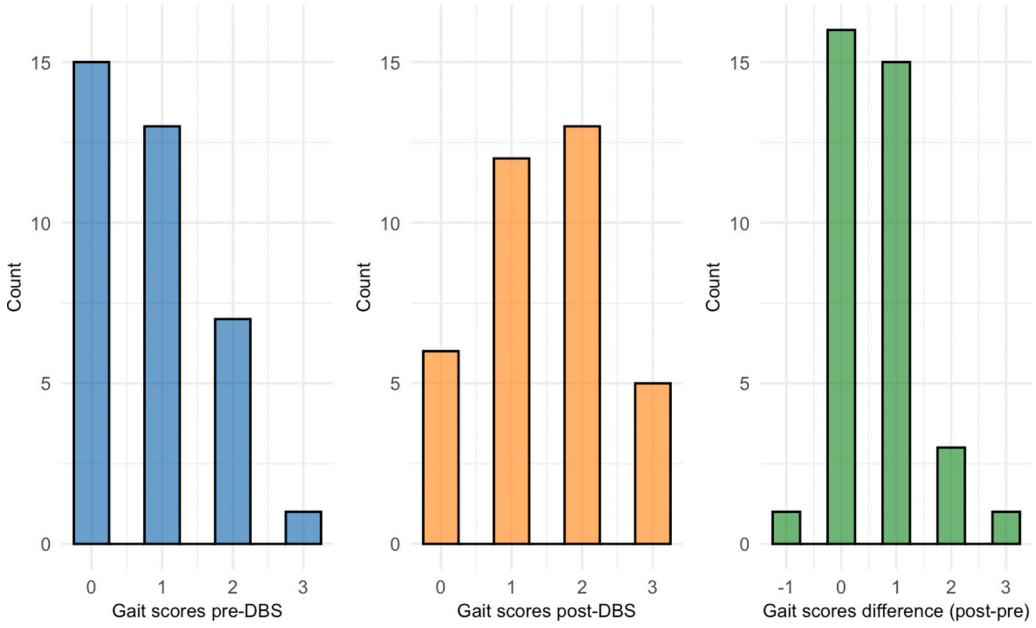

Fig. 1. Histograms of gait scores. In blue the gait scores pre-DBS surgery, in orange the gait scores 6–12 months post-DBS surgery and in green the difference between post and pre DBS gait scores.

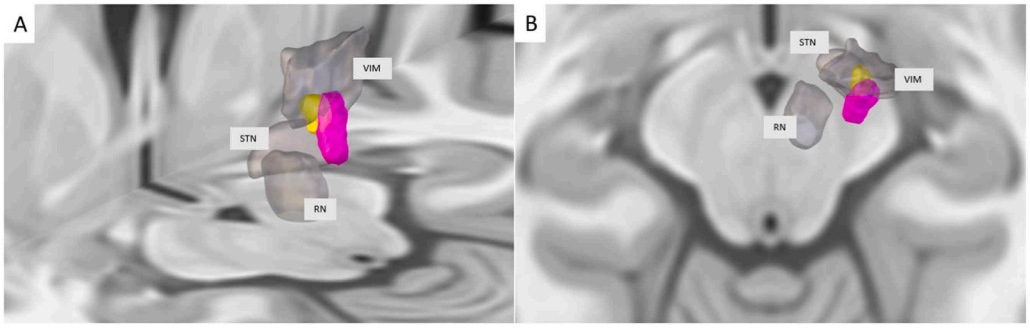

Fig. 2. Average stimulation area of eighty electrodes (N-map). This figure illustrates a 3D reconstruction of deep brain stimulation (DBS) electrode placements. The N-map (pink), shown in panels A (posteromedial perspective) and B (top-down view), depicts an activation map that includes all voxels stimulated by at least 4 volumes of tissue activated (VTAs) across the full cohort in the right hemisphere. This cumulative map highlights the total volume of tissue influenced by stimulation and partly overlaps with the sweetspot from Nowacki et al. (yellow) [15]. RN = red nucleus; STN = subthalamic nucleus, VIM = ventralis intermedius nucleus.

association (highest $\log_{10}$(p-values)) in both maps are centrally located within the respective VTAs and appear to be located in the same region. When comparing voxel-wise stimulation to the respective group mean scores (H_0=μ), no statistically significant area was identified for tremor improvement or for gait impairment. This suggests that no distinct anatomical region was associated to greater-than-average clinical benefit or adverse effect in this cohort.

3.3. Stimulation parameters and clinical outcomes

With the logistic mixed-effects model we identified a significant positive association between baseline gait ataxia and the likelihood of postoperative gait deterioration based on standard model estimates ($\beta = 16.69$, $p < .001$), suggesting that individuals with more severe baseline gait ataxia are more likely to experience deterioration in SARA score after DBS surgery. However, parametric bootstrapping with 1000 resamples yielded a wide 95% confidence interval (–0.34–26.22), which included zero, indicating that this effect may not be robust. Neither age, stimulation location nor distance to the DRTT significantly predicted gait deterioration in the model (see Table 2). See the supplementary material for comparisons of active contact locations in subject space and MNI space.

Secondly, a linear mixed-effects model was applied to evaluate predictors of tremor improvement using the same fixed and random effects. The analysis revealed a negative association between baseline gait ataxia and tremor improvement ($\beta = -0.14$, $p = 0.04$), indicating that greater baseline gait ataxia was linked to less improvement in tremor. The gait score difference was also significant ($\beta = -0.13$, $p = 0.048$, see Table 2), suggesting that greater gait deterioration may also be associated with reduced tremor improvement. In addition, the distance between the center of gravity of the DRTT and the active contact points showed a significant negative association ($\beta = -0.07$, $p = 0.04$), meaning that closer proximity to the DRTT corresponds to higher tremor improvement. No other predictors were found to have significant associations with tremor improvement (see Table 2).

To account for subject-level variability because each patient contributed data from two electrodes, both models included a random intercept for patients. In the gait impairment model substantial between-subject variability was observed (variance = 3688, SD = 60.73), whereas the model of tremor improvement showed low variability (variance = 0.016, SD = 0.13). Despite the difference in magnitude, which can be attributed to the distinct outcome scales, the inclusion of random effects in both models was justified to account for the non-independence of observations.

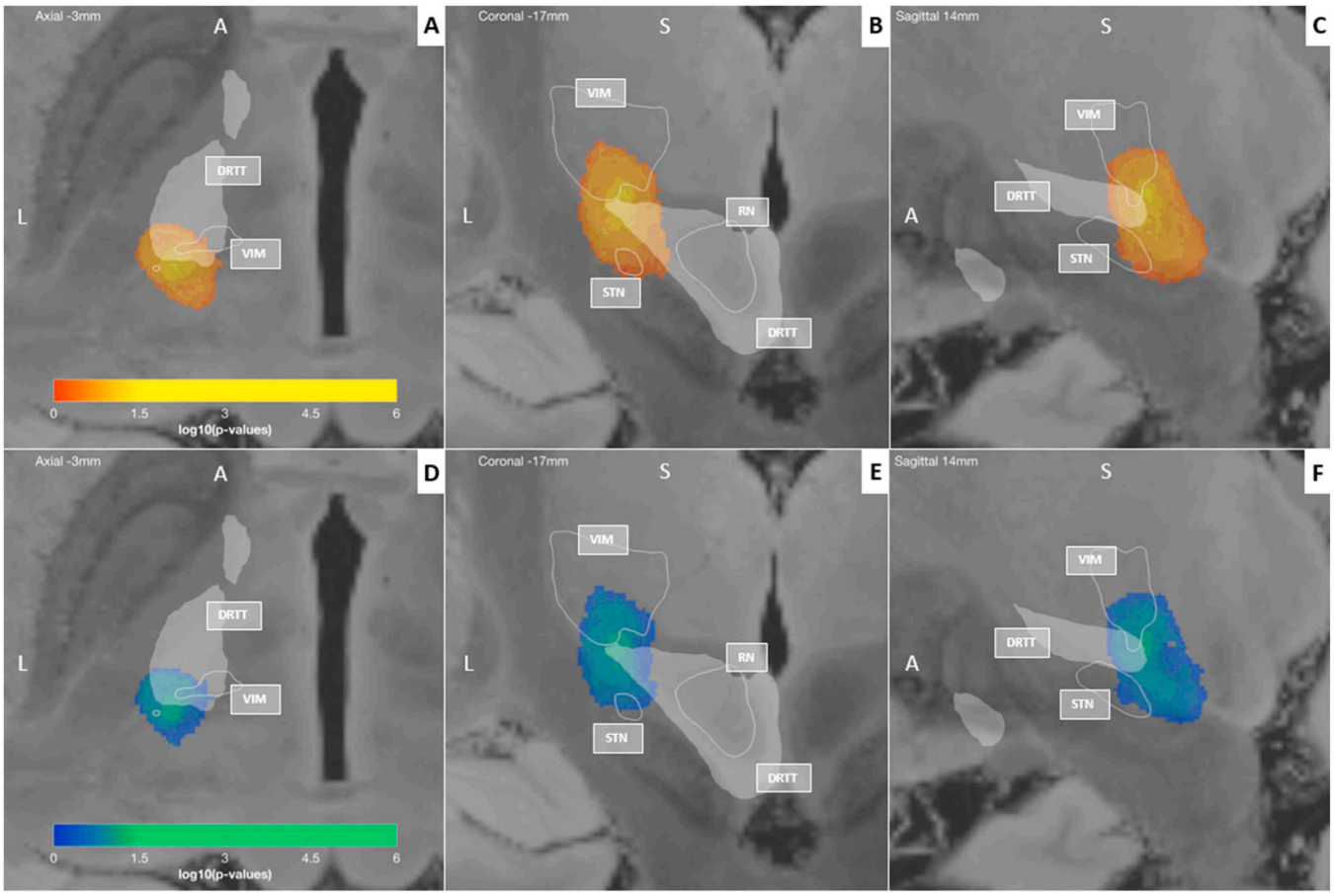

Fig. 3. Voxel-wise significance maps for tremor improvement and gait impairment. This figure displays brain regions significantly associated with tremor improvement (A–C) and gait impairment (D–F) in axial, coronal and sagittal views. Color gradients represent the strength of association: red (low) to yellow (high) for tremor improvement and blue (low) to green (high) for gait impairment. Both maps are localized to overlapping regions encompassing the ventral intermediate nucleus (VIM), posterior subthalamic area (PSA) and dentato-rubro-thalamic tract (DRTT). A = anterior; L = lateral; RN = red nucleus; STN = subthalamic nucleus; S = superior.

Table 2
Mixed-effects regression models for gait impairment (logistic) and tremor improvement (linear) in relation to stimulation location and distance to the dentato-rubro-thalamic tract (DRTT).

Variable	Estimate	SE	p	95% CI (bootstrapped)	Estimate	SE	p	95% CI
	Gait impairment				*Tremor improvement*			
Intercept	-6.76	22.98	0.77	[-55.98, 22.86]	4.70	0.22	< 0.001	[4.24, 5.12]
Age	0.76	3.25	0.82	[-25.67, 14.99]	-0.014	0.075	0.86	[-0.15, 0.13]
Baseline gait ataxia	16.68	3.73	**< 0.001**	[-0.25, 30.01]	-0.14	0.066	**0.039**	[-0.27, −0.02]
Stimulation location (PSA vs. VIM)	0.32	3.59	0.93	[-16.96, 20.13]	0.2	0.15	0.2	[-0.09, 0.49]
Distance to DRTT	0.34	0.94	0.72	[-1.76, 2.54]	-0.066	0.031	**0.039**	[-0.12, 0.001]
Tremor improvement	2.22	4.41	0.62	[-3.76, 10.81]	x	x	x	x
Gait score difference	x	x	x	x	-0.13	0.064	**0.048**	[-0.25, 0.01]

Finally, TEED was not associated with either gait impairment or tremor improvement (Table 3). Consistent with the previous model, baseline gait ataxia was again significantly associated with gait impairment. However, after bootstrapping again this result seemed not

Table 3
Mixed-effects regression models for gait impairment (logistic) and tremor improvement (linear) in relation to total electrical energy delivered (TEED).

Variable	Estimate	SE	p	95% CI (bootstrapped)	Estimate	SE	p	95% CI
	Gait impairment				*Tremor improvement*			
Intercept	-28.52	31.99	0.37	[-98.96, 12.99]	4.27	0.062	< 0.001	[4.16, 4.39]
Age	0.34	3.09	0.91	[-25.08, 23.18]	-0.019	0.079	0.81	[-0.17, 0.13]
Baseline gait ataxia	15.82	4.39	**< 0.001**	[-0.97, 35.56]	-0.13	0.068	0.063	[-0.26, −0.004]
TEED	1.64	2.75	0.55	[-3.33, 10.82]	-0.044	0.061	0.48	[-0.16, 0.078]
Tremor improvement	7.16	6.91	0.30	[-1.13, 22.18]	x	x	x	X
Gait score difference	x	x	x	x	-0.12	0.065	0.071	[-0.24, −0.0002]

robust (confidence interval [-0.25, 30.01]). Overall, this indicates that TEED does not explain variance in the outcomes beyond established clinical predictors.

Estimates (β), 95% confidence intervals (CI), standard errors (SE), and p-values are reported for each predictor. Models include fixed effects (age, baseline gait ataxia, stimulation location, distance to dentato-rubro-thalamic tract (DRTT), tremor improvement or gait score difference) and a random effect (patient). Dependent variables are change in gait ataxia (gait impairment model) and percent tremor improvement from baseline (tremor improvement model). Statistically significant predictors are shown in bold.

Estimates (β), 95% confidence intervals (CI), standard errors (SE), and p-values are reported for each predictor. Models include fixed effects (age, baseline gait ataxia, total electrical energy delivered (TEED), tremor improvement or gait score difference) and a random effect (patient). Dependent variables are change in gait ataxia (gait impairment model) and percent tremor improvement from baseline (tremor improvement model). Statistically significant predictors are shown in bold.

4. Discussion

Our analyses revealed substantial overlap between stimulation areas associated with tremor improvement and those linked to gait impairment. Notably, we did not identify a distinct area associated exclusively with either outcome. Mixed effects models revealed that stimulation location, or distance to the DRTT could not be associated to gait impairment in our sample. However, tremor improvement was negatively associated with distance to the DRTT, meaning that smaller distances to the DRTT correspond to more tremor improvement. Moreover, patients with higher baseline gait ataxia scores were more likely to exhibit gait impairment, although this did not remain significant after bootstrapping. Our findings align with previous reports suggesting that regions implicated in gait disturbances are closely situated to, or overlap with, those responsible for tremor control. This suggests that additional measures, such as structural and functional connectivity, should be considered rather than relying solely on simple anatomic targeting.

Previous studies have suggested more inferior stimulation within the PSA is associated with gait impairment [10,11]. However, these findings are based on comparisons between relatively small groups of patients with and without gait impairment or on whether the active contact was located in the VIM versus the PSA. Our results demonstrate a substantial overlap of the hotspots for both tremor improvement and gait impairment within and above the PSA, near the VIM, along the DRTT trajectory. Reich et al. observed that, in ET patients with ataxia, the mean VTA location was situated more medial and caudally in the PSA, potentially leading to stimulation of fibers involved in axial control [10]. However, as mentioned before, this study was limited by a small sample size (N = 5 per group) and relied on group-level comparisons of mean VTA locations. In our study, we employed a large cohort and conducted voxel-wise analyses, correlating individual stimulation regions with continuous measures of tremor improvement and gait impairment, thereby offering increased spatial specificity. Earlier research, including a study by Groppa et al., suggested vestibulo-cerebellar-thalamic afferents and the cerebello-rubrospinal network may be recruited through supratherapeutic stimulation at higher amplitudes [10,12]. Our group-level findings do not support this, as we observed no association between TEED and DBS-induced gait impairment, and the maps of tremor improvement and gait impairment showed considerable overlap. We did observe that the distance to the DRTT was significantly associated with tremor improvement, with closer proximity corresponding to greater benefit, consistent with previous findings by Dembek et al. [7,8]. In contrast, distance to the DRTT was not associated with gait impairment, suggesting that the DRTT may not be the primary determinant of DBS-induced gait changes. Nevertheless, involvement of more diffuse DRTT stimulation cannot be excluded, and using a single gait score for both hemispheres may have obscured subtle associations. Overall, while proximity to the DRTT influences tremor improvement, a relationship with gait impairment was not observed. Our comparison of active contact locations in subject space and MNI space revealed discrepancies between the two coordinate spaces, which may have affected the group-level results (in MNI space) by reducing their spatial specificity (see Supplementary material). These results do not exclude a potential involvement of differential fibers within the DRTT in DBS-induced gait impairment, underscoring the importance of future studies using patient-specific functional and structural network analyses to delineate the relevant pathways.

Given that the cerebellum, ventrolateral nucleus of the thalamus (including the VIM), and primary motor cortex all exhibit a somatotopic organization, it is plausible that fibers within the DRTT also maintain a distinct somatotopic arrangement [29–31]. Supporting this idea Al-Fatly et al. demonstrated a somatotopic organization within the CTC network, identifying functional networks associated with head versus hand tremor suppression that mapped to somatotopically distinct regions of the cerebellum and motor cortex [32]. This raises the possibility that specific tracts within the CTC may connect to regions responsible for lower extremity control, potentially explaining their role in DBS-induced gait impairment. Complementary findings by Fenoy et al. demonstrated that patients with DBS-induced ataxia exhibited reduced functional connectivity between the cerebellum and cortical regions, including the precentral gyrus and superior and inferior parietal lobules, when compared to patients without ataxia [33]. These regions could be used as regions of interest in a functional or structural network analysis to identify more specifically the fibers contributing to side effects. Relying solely on VTAs to localize regions associated with gait impairment may be too simplistic, as different subregions within a single VTA could contribute unequally to side effects due to somatotopic organization within the DRTT/CTC network. In our analysis each VTA was assigned a single uniform value for tremor improvement and gait impairment. To more accurately localize the regions responsible for side effects, we propose combining functional and structural network analyses.

Pre-existing gait ataxia or underlying disease progression may significantly contribute to post-surgical gait impairments. Chiu et al. previously reported that patients with greater baseline ataxia were more likely to develop DBS-induced gait disturbances (8). Our findings support this association, although the significance did not hold after bootstrapping. We were unable to confirm other reported risk factors, such as older age. A relationship between DBS-induced gait-impairment and shorter disease duration could not be tested due to substantial missing data [9]. These factors should be considered in future studies.

5. Limitations

The results of our study should be interpreted with some caution. Firstly, in our center, most patients are implanted with bilateral electrodes. Due to the retrospective nature of this study, assessment of gait per electrode separately was not available. This has limited our analysis to ascertaining a single gait score to both hemispheres. On the other hand, gait-impairment is more often encountered with bilateral stimulation [11], and previous studies have used a similar approach [32]. Secondly, assessment of gait impairment with item 1 of the SARA poses limitations. Although the SARA was designed to assess cerebellar ataxia, no reliable distinction can be made regarding the nature of the gait impairment based on this score, for example originating from a cerebellar, pyramidal or proprioceptive deficit. Furthermore, gait scores were slightly skewed to the left and our sample did not contain patients with severe gait impairment, with most patients exhibiting only mild gait impairment. A more heterogeneous sample including patients with more severe gait impairment could yield different results. Hence, in future studies the complete SARA protocol should be conducted and ideally assessed for each electrode separately. Thirdly, algorithms

implemented in Lead-DBS to reconstruct electrodes in MNI space may impact the spatial accuracy of electrodes (see Supplementary material for a comparison between electrode reconstructions in subject space and MNI space). As a result, our findings, and group-level analyses in general, should be interpreted with caution and not be applied directly for individual targeting. In addition, comprehensive comparison of VIM versus PSA tremor control outcomes remains challenging as standard T1 and T2 weighted imaging sequences available cannot definitively distinguish whether stimulation occurred at VIM or PSA level given their anatomical proximity. In current literature, PSA is variably reported at the level of the rubral wing (above the upper border of the RN) and at the level of widest diameter of the RN on T2-weighted imaging, two adjacent but distinct areas [34,35]. This inconsistency explains partially why comparisons between VIM and PSA outcomes can be difficult to interpret. Lastly, while our discussion suggests involvement of the DRTT, this remains tentative given the lack of tractography analyses and should be confirmed in future studies.

6. Conclusion

In this study, we examined the relationship between stimulation areas associated with tremor improvement and DBS-induced gait impairment, in a large cohort of 40 ET patients. Our findings revealed overlapping regions within the VIM, PSA and DRTT that were associated with both therapeutic effects and side effects. Consequently, no distinct region could be identified as being solely responsible for DBS-induced gait impairment. Notably, while proximity to the DRTT predicted tremor improvement, it was not associated with gait impairment, suggesting that gait-related side effects are not determined by DRTT distance alone. Nevertheless, a somatotopic organization within the DRTT and the broader CTC network could mean that stimulation of overlapping regions differentially affects tremor and gait depending on which fiber pathways are engaged. As relying solely on VTAs may oversimplify these relationships, further research integrating individual tractography and functional connectivity analyses is needed to elucidate the neural networks underlying DBS-induced gait impairment and refine stimulation strategies to minimize side effects while optimizing tremor control.

Funding

A.A. Boogaard was funded by research grants from ZonMW and Amsterdam Neuroscience. A.W.G. Buijink was funded by research grants from ZonMw and Stichting Bavalo.

Declaration of Competing Interest

PR Schuurman is independent consultant for Medtronic, Boston Scientific and Elekta. RMA de Bie received research grants from Medtronic, Bial, ZonMw, AMC Foundation, ROMO Foundation, and Stichting ParkinsonFonds, all paid to the institution. M Beudel received funding from an EU Joint Programme – Neurodegenerative Disease Research (JPND) project. The project is supported through the following funding organisations under the aegis of JPND – www.jpnd.eu: the Netherlands Organisation for Health Research and Development (ZonMw) – The Netherlands. M Bot received research grants from ZonMw and Amsterdam Neuroscience, all paid to the institution. AWG Buijink received research grants from ZonMw and Stichting Bavalo, all paid to the institution.

Acknowledgements

The authors gratefully acknowledge Till Dembek and Christina van der Linden for their support in creating the figure illustrating stimulation maps.

Appendix A. Supporting information

Supplementary data associated with this article can be found in the online version at doi:10.1016/j.jdbs.2026.05.001.

References

[1] Louis ED, McCreary M. How common is essential tremor? Update on the worldwide prevalence of essential tremor. Tremor Other Hyperkinet Mov (N Y) 2021;11:28.
[2] Deuschl G, et al. Treatment of patients with essential tremor. Lancet Neurol 2011; 10(2):148–61.
[3] Buijink AW, et al. Motor network disruption in essential tremor: a functional and effective connectivity study. Brain 2015;138(Pt 10):2934–47.
[4] Coenen VA, et al. Modulation of the cerebello-thalamo-cortical network in thalamic deep brain stimulation for tremor: a diffusion tensor imaging study. Neurosurgery 2014;75(6):657–69. discussion 669–70.
[5] Middlebrooks EH, et al. Structural connectivity-based segmentation of the thalamus and prediction of tremor improvement following thalamic deep brain stimulation of the ventral intermediate nucleus. Neuroimage Clin 2018;20: 1266–73.
[6] Holslag JAH, et al. Deep Brain Stimulation for Essential Tremor: A Comparison of Targets. World Neurosurg 2018;110:e580–4.
[7] Dembek TA, et al. PSA and VIM DBS efficiency in essential tremor depends on distance to the dentatorubrothalamic tract. Neuroimage Clin 2020;26:102235.
[8] Middlebrooks EH, et al. Connectivity correlates to predict essential tremor deep brain stimulation outcome: Evidence for a common treatment pathway. Neuroimage Clin 2021;32:102846.
[9] Chiu SY, et al. Ataxia and tolerance after thalamic deep brain stimulation for essential tremor. Park Relat Disord 2020;80:47–53.
[10] Reich MM, et al. Progressive gait ataxia following deep brain stimulation for essential tremor: adverse effect or lack of efficacy? Brain 2016;139(11):2948–56.
[11] Kim MJ, et al. Stimulation-Induced Side Effects of Deep Brain Stimulation in the Ventralis Intermedius and Posterior Subthalamic Area for Essential Tremor. Front Neurol 2021;12:678592.
[12] Groppa S, et al. Physiological and anatomical decomposition of subthalamic neurostimulation effects in essential tremor. Brain 2014;137(Pt 1):109–21.
[13] Buijink AWG. Chapter 13 - Optimizing parameter adjustment in tremor. Learn Deep Brain Stimul Manag Clin Cases 2024:167–79.
[14] Sajonz BEA, et al. Disbalanced recruitment of crossed and uncrossed cerebello-thalamic pathways during deep brain stimulation is predictive of delayed therapy escape in essential tremor. Neuroimage Clin 2024;41:103576.
[15] Nowacki A, et al. Probabilistic Mapping Reveals Optimal Stimulation Site in Essential Tremor. Ann Neurol 2022;91(5):602–12.
[16] Fahn, S., *Clinical rating scale for tremor*, E. Tolosa, Editor. 1993: Parkinson's disease and movement disorders. p. 271–280.
[17] Schmitz-Hübsch, T., Scale for the assessment and rating of ataxia: Development of a new clinical scale., S.T. Du Montcel, Editor. 2006: Neurology. p. 1717–1720.
[18] Anderson CJ, et al. Neural selectivity, efficiency, and dose equivalence in deep brain stimulation through pulse width tuning and segmented electrodes. Brain Stimul 2020;13(4):1040–50.
[19] McAuley MD. Incorrect calculation of total electrical energy delivered by a deep brain stimulator. Brain Stimul 2020;13(5):1414–5.
[20] Holewijn RA, et al. Implementation of Intraoperative Cone-Beam Computed Tomography (O-arm) for Stereotactic Imaging During Deep Brain Stimulation Procedures. Oper Neurosurg (Hagerstown) 2020;19(3):E224–9.
[21] Horn A, Kuhn AA. Lead-DBS: a toolbox for deep brain stimulation electrode localizations and visualizations. Neuroimage 2015;107:127–35.
[22] Horn A, et al. Lead-DBS v2: Towards a comprehensive pipeline for deep brain stimulation imaging. Neuroimage 2019;184:293–316.
[23] Avants BB, et al. Symmetric diffeomorphic image registration with cross-correlation: evaluating automated labeling of elderly and neurodegenerative brain. Med Image Anal 2008;12(1):26–41.
[24] Friston KJ. Statistical parametric mapping. Elsevier; 2007.
[25] Husch A, et al. PaCER - A fully automated method for electrode trajectory and contact reconstruction in deep brain stimulation. Neuroimage Clin 2018;17:80–9.
[26] Horn A, et al. Probabilistic conversion of neurosurgical DBS electrode coordinates into MNI space. Neuroimage 2017;150:395–404.
[27] Brainlab, *Elements Trajectory Planning [software]*. 2025, Brainlab SE: Munich, Germany.
[28] Team, R., *RStudio: Integrated Development for R*. 2020: Boston.
[29] Vitek JL, et al. Physiologic properties and somatotopic organization of the primate motor thalamus. J Neurophysiol 1994;71(4):1498–513.
[30] Buckner RL, et al. The organization of the human cerebellum estimated by intrinsic functional connectivity. J Neurophysiol 2011;106(5):2322–45.
[31] Penfield W, Boldrey E. Somatic motor and sensory representation in the cerebral cortex of man as studied by electrical stimulation. Brain 1937:389–443.
[32] Al-Fatly B, et al. Connectivity profile of thalamic deep brain stimulation to effectively treat essential tremor. Brain 2019;142(10):3086–98.

[33] Fenoy AJ, et al. Evaluating functional connectivity differences between DBS ON/OFF states in essential tremor. Neurotherapeutics 2024;21(4):e00375.
[34] Bot M, et al. The Fast Gray Matter Acquisition T1 Inversion Recovery Sequence in Deep Brain Stimulation: Introducing the Rubral Wing for Dentato-Rubro-Thalamic Tract Depiction and Tremor Control. Neuromodulation 2023;26(8):1705–13.
[35] Sun X, et al. Bilateral Posterior Subthalamic Area Deep Brain Stimulation for Essential Tremor: A Case Series. Front Hum Neurosci 2020;14:16.